Modern design tools and a new paradigm in optical coating design

Alexander V. Tikhonravov[1,*] and Michael K. Trubetskov[1,2]

[1]Research Computing Center, Moscow State University, Leninskie Gory, Moscow 119991, Russia

[2]Max Planck Institute of Quantum Optics, Hans-Kopfermann-Strasse 1, Garching 85748, Germany

*Corresponding author: tikh@srcc.msu.ru

Received 7 August 2012; revised 11 September 2012; accepted 12 September 2012; posted 13 September 2012 (Doc. ID 173978); published 17 October 2012

Several modern optical coating designs tools are discussed in the frame of a new design paradigm proposing the search not for a formally optimal solution with the lowest possible merit function value but for the most practical solution that takes into account additional feasibility demands. Considered design tools include a stochastic optimization procedure that takes into account upper and lower constraints for layer optical thicknesses. This procedure allows one to obtain multiple solutions to a design problem, which presents additional opportunities for choosing a practically optimal design. Two special design techniques involving integer optimization also take into account additional demands. The first one is aimed at designing multicavity narrow bandpass filters with quarter wave or multiple quarter wave layer optical thicknesses. It enables obtaining bandpass filters with extremely steep transmittance slopes, bandwidths of several tens of nanometers, and very small ripples in transmission zones. The second technique is aimed at covering design problems that have been traditionally solved using the theory of equivalent layers. One more technique considered in this paper is aimed at reducing the influence of noncorrelated thickness errors on design spectral characteristics.

OCIS codes: 310.4165, 310.5696, 310.6805.

1. Introduction

The history of computer-aided tools for optical coatings design can be traced back more than half a century, and its first decades can be found in several texts on thin film optics [1–6]. The most noticeable trends in the development of design tools during the first part of this period were attempts to find a general purpose design approach that was capable of solving design problems of very different types and implementations of various mathematical optimization routines for computational designing of optical coatings. These trends were recognized by Dobrowolski, who proposed subdivision of optical coating design tools into synthesis and refinement design techniques [7].

Before the end of the 1980s, an amazingly wide circle of design problems was addressed by the design approach based on the equivalent layers theory. To a great extent the success of this approach should be attributed to Thelen, who summarized specific details of its implementation and a great number of designs for practically all known applications in his book, published in 1988 [2]. A wide range of applications was addressed also by the Fourier transform syntheses method [8–15]. In parallel with the development of synthesis techniques, experience in implementing various refinement techniques was accumulated [16], and these techniques were implemented within various synthesis methods [17]. Nowadays all modern synthesis methods incorporate one or more mathematical local optimization routines as their integral parts [18].

A demand for a general purpose synthesis method was a main motivation for the invention of the needle

1559-128X/12/307319-14$15.00/0

optimization technique [19]. Because of physically sensible basic concepts and an accurate mathematical formalism of their implementation, this technique was found to be an effective tool for solving design problems of any complexity [20,21]. The most powerful gradual evolution version of the needle optimization technique [21] is based on the recognition of a key role of design total optical thickness. The importance of this parameter was underlined by Dobrowolski in several publications. In [22] he mentioned that "a certain minimum overall optical thickness is required for a solution to a given problem no matter what design method is employed." Eleven years later he wrote that solutions to problems with several diverse types of quantities of interest require, as a rule, systems with large overall thickness [7]. Nevertheless a key role of design total optical thickness was entirely recognized only recently. As a result, the concept of three main design parameters, namely merit function value *MF*, number of design layers *N*, and design total optical thickness *TOT*, was introduced [23].

The gradual evolution version of the needle optimization technique is the only design technique that in a quite natural and physically sensible way constructs a set of designs with decreasing *MF* values and increasing *N* and *TOT* values. This technique enables one to obtain designs with extremely low merit function values [21]. However such designs are not necessarily the best designs because they may be unreasonably complex for a practical implementation [24]. As a result of successful application of gradual evolution technique to various design problems, a new paradigm in optical coating design has been formulated [25]. On the contrary, with searching for a formally optimal design with the lowest possible merit function value, this paradigm proposes for one to find a practically optimal design with the most reasonable combination of all design parameters. It is impossible to formalize the concept of a practically optimal design because its choice depends on too many factors. Nevertheless, main quantitative factors and basic considerations that should be taken into account can be outlined. First of all, instead of a merit function value as a single parameter characterizing a quality of the design, one should consider the three main design parameters listed above, i.e., *MF*, *N*, and *TOT*. Selection of a practically optimal design starts with the choice of their reasonable combinations. It is then necessary to take into account various practical considerations, including potentialities of available production and monitoring equipment, estimations of production costs, additional application demands, etc.

The new paradigm has been implicitly applied by many researchers whose publications help to recognize its importance. An excellent example is the design of antireflection (AR) hard coatings for plastic substrates [26–28]. The AR hard designs take into account an additional demand of coating hardness that, for such designs, corresponds to the hardness of single SiO_2 layers [26]. They are structurally different from standard "optimal" AR designs [24] and consist of many thin high-index layers spaced by much thicker low-index SiO_2 layers.

Another example is a three-component broadband normal incidence AR coating proposed in [29]. According to the maximum principle, in thin film optics [30] at the normal light incidence the lowest *MF* values are achieved by the two-component designs with the maximum and minimum values of layer refractive indices. In [29], a formally optimal two-component AR design was compared with a three-component design derived by a special reduction procedure from an "optimal" 14-layer two-component design. Based on multiple computational manufacturing experiments with different types of simulated production errors, it was clearly demonstrated that a practically optimal design is the three-component one.

Choosing a practically optimal design from a series of theoretical designs with the help of computational manufacturing experiments becomes a common approach [29, 31–35]. In this paper we do not discuss specific details of this approach but concentrate our attention on new developments in design techniques that extend researchers opportunities in constructing a series of designs for a subsequent choice of the most practical one. In [7], Dobrowolski indicated that it is desirable to have access to various thin film synthesis methods because different methods can provide different designs, and depending on the available equipment and deposition process, one design may be easier to produce than another. That is why new developments in design techniques are still important and are entirely consistent with the new design paradigm. In Section 2 we discuss the design approach that allows one to take into account lower and upper constraints for layer thicknesses. In Section 3 specific design techniques involving integer optimization are discussed. These techniques can be used for designing some types of filters with additional feasibility demands to their parameters. In Section 4 the design approach aimed at reducing the influence of noncorrelated thickness errors is presented. Final conclusions are provided in Section 5.

2. Design Approach Taking into Account Lower and Upper Constraints for Layer Thicknesses

Taking into account layer thickness constraints can be an important additional demand for choosing a practically optimal design. There may be practically proved lower limits for physical layer thicknesses for conventional deposition processes [29]. Such limits are always present in design problems for extreme-ultraviolet and x-ray applications where coating layer thicknesses are already small and it is practically impossible to deposit layers thinner than several atomic layers. Lower thickness limits can be applied in connection with monitoring strategies used for coating production. For example active monochromatic monitoring strategies involving

corrections of termination levels require that at least one monitoring signal extremum is registered during a layer deposition [36–39]. This is possible only if a monitored layer is thick enough.

The exceptional importance of a coating total optical thickness has already been underlined several times. Nevertheless it may be desirable to apply upper limits for thicknesses of individual layers. For example, with a large film thickness, essential changes of film structure can take place [6]. Upper constraints for individual layer thicknesses may also help to avoid unreasonably high total optical thickness values.

Below we assume that lower and upper constraints are applied to all layer thicknesses. To describe the design approach taking into account these constraints, we consider two design problems. The first one is designing a three-line filter with narrow transmission zones near 450, 510, and 650 nm. The widths of these zones should be close to 10 nm, and there should be steep transmittance slopes between transmission and rejection zones. Target transmittance for this filter is specified as 100% in the spectral zones 445–455 nm, 505–515 nm, 635–645 nm with 1 nm wavelength step and as 0% in the spectral zones 400–440 nm, 460–500 nm, 520–630 nm, 650–700 nm, also with 1 nm wavelength step. The second problem is designing a hot mirror with target transmittance of 100% in the 400–690 nm zone and target transmittance of 0% in the 710–1200 nm zone. The wavelength step for target specification is 2 nm in both zones. For both design problems we assume that lower and upper constraints for layer optical thicknesses are 100 and 350 nm, substrate refractive index is 1.52, incident medium is air, and high and low refractive indices are 2.35 and 1.45. Merit functions for the design problems are specified in a standard way [21] as

$$MF = \left\{ \frac{1}{L} \sum_{j=1}^{L} \left[\frac{T(\lambda_j) - \hat{T}(\lambda_j)}{\Delta T_j} \right]^2 \right\}^{1/2}, \qquad (1)$$

where the summation is performed over the specified wavelength grid, L is the total number of wavelength grid points, $T(\lambda)$ is the design transmittance, $\hat{T}(\lambda)$ is the target transmittance, and ΔT_j are transmittance tolerances. It should be noted that other forms of the merit function representation can also be used. For example, instead of a wavelength grid with evenly distributed wavelength points it is possible to use a spectral grid with equidistant wavenumber points. However, a specific form of the wavelength grid is not essential for our further considerations, and in the following text we consider merit functions of the above discussed type.

Below we assume 1% tolerances. With such tolerance values the merit function represents a root mean square deviation of the design transmittance from the target transmittance in percentage.

The design process starts with the application of the gradual evolution version of the needle optimization technique [21]. A set of designs constructed by the gradual evolution design procedure is used for estimating a complexity of design required for achieving a desired merit function value. It is reasonable to start this procedure just from a boundary between incident medium and substrate, i.e., with no starting design at all. Figure 1 illustrates several intermediate steps of designing of the three-line filter. It presents *MF* and *N* values for the 50 designs with *TOT* values between 6000 and 12,000 nm. As expected, in general *MF* values decrease and *N* values increase with growing *TOT* values.

As an illustration, spectral transmittance and layer optical thicknesses of one of the designs obtained by the gradual evolution procedure are shown in Fig. 2. Its main design parameters are $MF = 0.191$, $N = 75$, and $TOT = 9687.5$ nm. This design has excellent spectral properties (see the left part of Fig. 2). However, 15 design layers have optical thicknesses below 100 nm. Other designs constructed by the gradual evolution procedure also have layers thinner than 100 nm.

There are special procedures that allow one to exclude thin design layers and to decrease the total number of layers at the expense of merit function increase [21,23]. However, it may be difficult to fulfill thickness constraints requirements for all layers, especially if they are tough, as in the considered examples. For this reason, at the next step we apply a specially adopted stochastic optimization procedure that directly takes into account thickness constraints. This procedure performs multiple optimizations of designs with a fixed number of design layers in a bounded thickness domain specified by the applied constraints. Results of the gradual evolution procedure are used to set the number of design layers and to generate thicknesses of random starting designs.

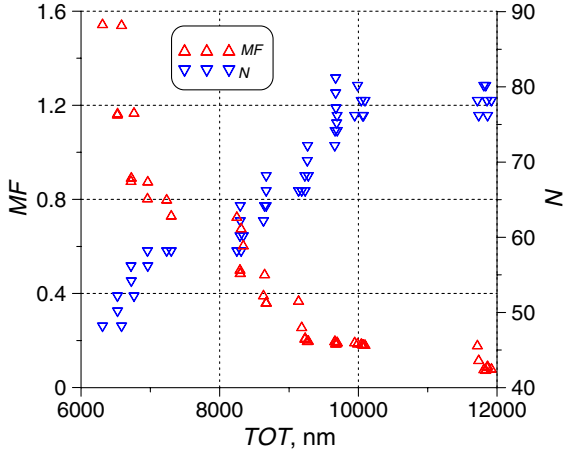

Fig. 1. (Color online) Main parameters (*N*, *MF*, *TOT*) of the 50 intermediate three-line filter designs obtained by the gradual evolution procedure.

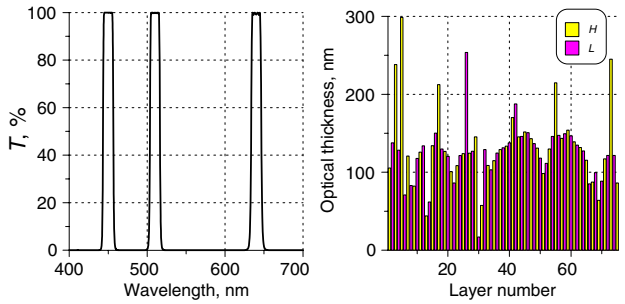

Fig. 2. (Color online) Spectral transmittance (left) and layer optical thicknesses (right) of the three-line filter design with $N = 75$, $MF = 0.191$, $TOT = 9687.5$ nm obtained by the gradual evolution procedure.

There is one more reason for application of the stochastic design procedure. It was already demonstrated that many design problems have multiple solutions with close combinations of three main design parameters: *MF*, *N*, and *TOT* [21]. Obviously constructing multiple solutions presents additional opportunities for choosing a practically optimal design. The proposed stochastic design procedure is aimed at obtaining such solutions.

Results of the gradual evolution procedure enable one to estimate total optical thickness values required for achieving sufficiently low merit function values. According to Fig. 1, merit function values of 0.2–0.4 can be achieved with design total optical thickness values of around 9000 nm. We shall take this value as an estimation for *TOT*. For *TOT* values in the range 9000 ± 300 nm, numbers of design layers in Fig. 1 are between 62 and 72. Because *N* values can be usually decreased at the expense of some *MF* increase, for the stochastic optimization we shall fix the number of design layers at $N = 51$. Stochastic optimizations are performed with a large number of randomly generated starting designs that layer optical thicknesses are random values with the mathematical expectation of 175 nm. Thus the mathematical expectation of *TOT* values of 51-layer random starting designs is close to the estimated *TOT* value of 9000 nm.

Local optimizations of random starting designs can be performed using various local optimization routines, but to achieve the best possible performance one should apply analytical expressions for calculating merit function gradients and Hesse matrices [40]. Such local optimization methods as damped least squares (DLS), Newton method, quasi-Newton DLS, and sequential quadratic programming (SQP) [41] have been found especially efficient for constrained local optimizations in a bounded layer thickness domain. Unfortunately, as mentioned by Dobrowolski [7], there is no universal local optimization method providing the best possible convergence in all situations, and it is advisable to try various methods. In the considered case of a three-line filter, the SQP method is especially efficient. A local optimization of one 51-layer random starting design takes less than 1 s on a PC with 3 GHz dual-core processor. Because of this fact, thousands of stochastic optimizations can be performed in a reasonable time.

The goal of stochastic optimizations is to find a series of deep local minima in the bounded domain specified by thickness constraints (a series of solutions to design problem). To accelerate a search for such minima, the following iterative stochastic optimization procedure is useful. First M_0 local optimizations with random starting designs from a bounded thickness domain specified by thickness constraints are generated. Mathematical expectations for individual layer thicknesses of these random designs are TOT/*N*, where *TOT* and *N* are chosen as discussed above. Designs obtained by local optimizations are collected and ordered in accordance with the achieved merit function values. Let X_0 be a vector of design layer optical thicknesses and MF_0 be a merit function value of the best collected design. When the first series of local optimizations is finished, the next series of M_1 optimizations is performed. Starting designs for this series are generated around X_0 using a generator of normally distributed values so that mathematical expectations of layer optical thicknesses are equal to respective coordinates of vector X_0 and their standard deviations are proportional to these coordinates with a coefficient of proportionality σ. When the second series is finished, the best achieved merit function value MF_1 is compared with MF_0, and if it is less than MF_0, the vector X_0 is replaced by the new vector X_1, providing so far the best *MF* value. The process is repeated in the same way *K* times, where *K* is a parameter of the discussed stochastic procedure. The final design is a design with the lowest merit function value found at all steps of the iterative procedure. When this procedure is finished, it may be started again and a new solution to a design problem can be obtained. The existence of multiple solutions is demonstrated below using the two design problems formulated at the beginning of this section.

For designing the three-line filter, the parameter M_0 was taken equal to 3000, the number of iterations *K* was 6, $M_1, \ldots, M_K$ values were 1000, and σ was taken equal to 3% for all iterations. The iterative stochastic optimization procedure was performed several times and always new solutions to the considered design problem were obtained. The main design parameters corresponding to 10 solutions are presented in Table 1. One can see that *TOT* values of these solutions are between 9202.9 and 9665.9 nm, i.e., they differ for no more than 5%. Achieved *MF* values are between 0.464 and 0.599. They are higher than the *MF* value of the 75-layer design with the transmittance shown in Fig. 2, but this is not surprising because, first of all, new designs have much smaller numbers of layers ($N = 51$) and also because there are additional thickness constraints applied to these designs. Nevertheless all obtained designs have excellent spectral properties and if plotted their

Table 1. Merit Function *MF* and Total Optical Thickness *TOT* Values of the 51-Layer Three-Line Filter Designs

Design	*MF*	*TOT*
1	0.526	9212.7
2	0.524	9363.9
3	0.516	9409.7
4	0.479	9422.8
5	0.571	9202.9
6	0.599	9391.2
7	0.570	9665.9
8	0.464	9371.8
9	0.524	9226.7
10	0.496	9382.7

transmittances will be practically nondistinguishable from that shown in the left part of Fig. 2.

Figure 3 presents layer optical thicknesses of the obtained designs. One can see that all designs are structurally different. In fact even more designs with $N = 51$, *MF*, and *TOT* values close to those indicated in Table 1 can be obtained. For the considered problem an existence of a large number of solutions with close combinations of three main design parameters has a physical explanation. In the case of single line narrow bandpass filters, an existence of multiple solutions has been demonstrated and physically explained in [42]. It was shown that all such filters are resonance multilayer structures with several resonance cavities. Narrow bandpass filter designs with close spectral properties may be structurally different because analogous spectral properties can be achieved by simultaneous variations of numbers of reflecting layers and orders of spacer layers [42]. Three line bandpass filters are also resonance structures that can be easily checked by plotting electric field distributions at transmission lines wavelengths of 450, 510, and 650 nm. A variety of solutions observed in Fig. 3 is connected with a variety of ways in which coating layers may form resonance cavities and surrounding groups of reflecting layers.

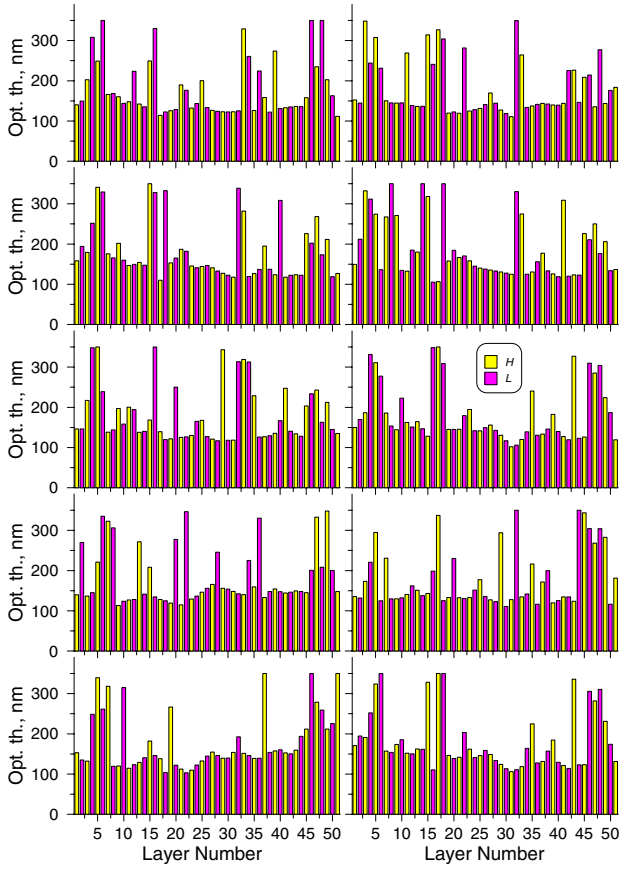

Fig. 3. (Color online) Layer optical thicknesses of the 10 three-line filter designs with $N = 51$, *MF* and *TOT* values indicated in Table 1.

As mentioned in the Section 1, in this paper we do not discuss modern approaches for choosing a practically optimal design from a variety of possible theoretical designs. Nevertheless, it is worthwhile to present some estimations demonstrating that designs with close parameters may have different feasibility properties. The most important effect that may prevent a successful application of direct broadband monitoring for optical coating production is a cumulative effect of thickness errors [43,44]. In [43], formulas for a preproduction estimation of this effect were derived. Figure 4 presents estimations of expected thickness errors for the Designs 2 and 3 from Table 1, where parameters are especially close. It is assumed that direct broadband monitoring measurements are performed in the spectral range from 400 to 900 nm with 1 nm wavelength step and with 0.5% random noise in transmittance measurement data. A cumulative effect of thickness errors is clearly observed for both designs. But for the last 20 layers it is much stronger in the case of Design 3. This suggests that Design 2 is more attractive from a practical point of view. However, for a more detailed comparison of feasibility properties of the obtained designs, one should perform a series of computational manufacturing experiments simulating a real production environment.

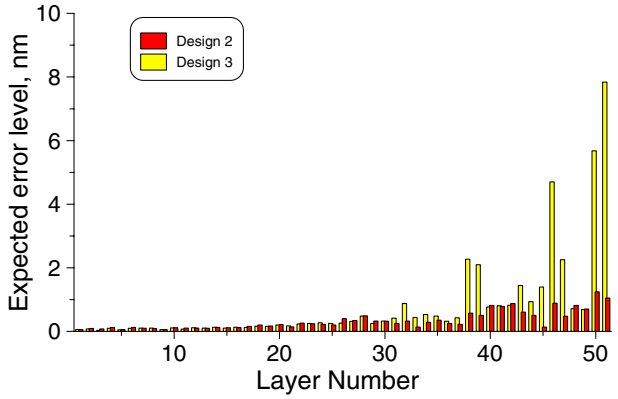

Fig. 4. (Color online) Preproduction estimation of thickness errors for the Designs 2 and 3 from Table 1 in the case of broadband monitoring in the 400–900 nm spectral range with 0.5% random noise in transmittance measurement data.

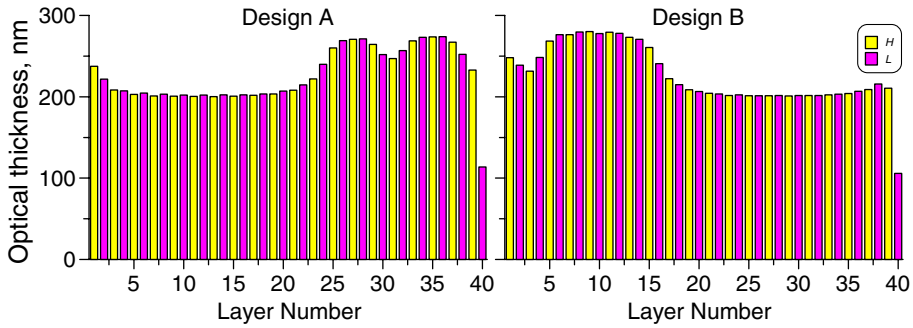

Fig. 5. (Color online) Layer optical thicknesses of the two hot mirror designs with $N = 40$ and $MF = 0.865$, $TOT = 9046.1$ nm (Design A) and $MF = 0.913$, $TOT = 9062.3$ nm (Design B).

The iterative stochastic optimization procedure with the same parameters as above was applied to designing of hot mirrors with target specifications indicated at the beginning of this section. Several designs of such mirrors with excellent spectral properties were presented in [21]. But all these designs had several thin layers with optical thicknesses of about 20–30 nm. It turns out that using nonconstrained optimization techniques, it is difficult to obtain hot mirror designs without such thin layers. Thus, for avoiding thin layers, constrained optimization techniques may be required.

Based on the results of [21], the number of layers for the stochastic optimization procedure was chosen equal to 40. As before, this procedure was performed several times but on the contrary with designing of the three-line filter it was usually converging to one of the two designs (Design A or Design B) with optical thicknesses presented in Fig. 5. For these designs their *TOT* values and achieved *MF* values are very close. They are indicated in the caption of Fig. 5. The transmittance of the Design A is presented in Fig. 6. The transmittance of the Design B is not plotted because it is nearly the same as that in Fig. 6.

Based on a steady convergence of the stochastic optimization procedure to one of the two designs depicted in Fig. 5, it is possible to conclude that for the chosen number of design layers and in the thickness domain specified by the applied constraints there are only two structurally different hot mirror designs that should be considered as candidates for choosing a practically optimal design. It should be noted that not necessarily a design with the lowest *MF* value will be the best one for a practical implementation. This is demonstrated by Fig. 7 presenting preproduction estimations of thickness errors for the designs from Fig. 5 in the case of direct broadband monitoring measurements with the same parameters as above. A cumulative effect of thickness errors is much less in the case of Design B which *MF* value is higher than *MF* value of the Design A.

3. Design Techniques Involving Integer Optimization

Specific design problems may require applications of special design techniques involving integer optimization. The most important example of such problems is designing of multicavity narrow bandpass filters, in particular filters for wavelength-division multiplexing (WDM) applications. The needle optimization technique allows designing of filters with excellent spectral properties, but these filters have layers with nonquarter wave optical thicknesses. At the same time, a special technique from [42] is aimed at designing of multicavity filters with quarter wave layer optical thicknesses, which allows one to explore an error self-compensation effect associated with turning point optical monitoring of production of filters with such layer thicknesses [45]. It was recently demonstrated [46] that this technique can be effectively used for designing of filters with steep transmittance slopes in visible spectral range. In the first part of this section we discuss the most recent modifications of the integer optimization technique originally proposed in [42].

Designing a narrow bandpass filter starts with specifications of its central wavelength, bandwidth of the transmission zone (for example, bandwidth at the −0.5 dB attenuation level), and bandwidth at the rejection level (for example, bandwidth at the −30 dB attenuation level). The ratio of specified bandwidth values is called a shape factor. This factor defines a steepness of transmittance slopes in the transition zones between transmission and rejection levels. Based on input data, the minimum number of filter

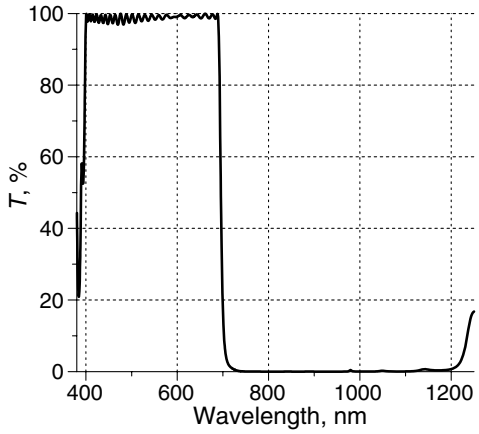

Fig. 6. Spectral transmittance of the hot mirror design with $N = 40$, $MF = 0.865$, $TOT = 9046.1$ nm (Design A).

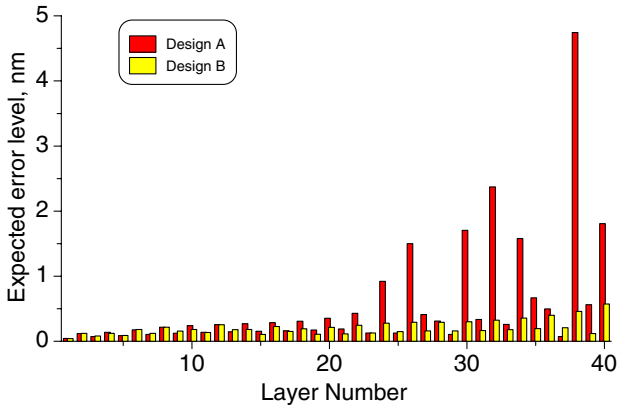

Fig. 7. (Color online) Preproduction estimation of thickness errors for the two hot mirror designs depicted in Fig. 5 in the case of broadband monitoring in the 400–900 nm spectral range with 0.5% random noise in transmittance measurement data.

cavities that are required to achieve a specified steepness is determined [42].

Let the number of filter cavities be equal to q. A general schematic of a narrow bandpass filter with q cavities can be presented as

$$M_1S_1M_2S_2M_3\ldots S_qM_{q+1}, \tag{2}$$

where $S_1,\ldots,S_q$ denote spacer layers forming filter cavities and $M_1,\ldots,M_{q+1}$ denote sequences of layers forming reflectors at both sides of spacer layers. In [42] quarter wave mirrors were considered as such reflectors.

Optical thicknesses of spacer layers are equal to $s\lambda_0/2$, where λ_0 is the filter's central wavelength and s is the order of the spacer layer. Denote $s_1,\ldots,s_q$ the orders of spacer layers, and $m_1,\ldots,m_{q+1}$ the numbers of layers of $M_1,\ldots,M_{q+1}$ mirrors. Integer parameters s_j, m_j are design parameters of the method of [42]. The design procedure starts with the specification of one of the possible filter prototypes that corresponds to the specification of starting values for the integer parameters s_j, m_j. After this, a specially adopted integer optimization procedure is applied and optimal values of these parameters are found. In the case of 3–5 filter cavities excellent results are obtained in fractions of a second.

With growing number of filter cavities, the number of variable integer parameters is growing, and it becomes more difficult to achieve a high flatness of spectral transmittance in the transmission zone, especially if this zone is wide. The modifications considered below extend designers' opportunities in constructing bandpass filters with extremely steep transmittance slopes, bandwidths of several tens of nanometers, and very small ripples in transmission zones. They are based on fundamental principles defining spectral properties of multicavity resonance structures. These principles were first investigated by the theory of microwave filters and then were successfully applied to designing of various types of thin film optical filters [6].

From a physical point of view, a spectral transmittance of a multicavity filter is defined by phase properties of filter cavities and reflectivities of mirrors surrounding these cavities (spacer layers). Reflectivities of mirrors depend on parameters m_j.

Phase properties of filter cavities are connected with parameters s_j as well as with phase shifts on reflections from surrounding mirrors. Consider one of the cavities. Its resonance properties are specified by the phase retardance

$$\varphi(\lambda) = \varphi_l(\lambda) + \varphi_r(\lambda) - 2\pi s\lambda_0/\lambda, \tag{3}$$

where s is a spacer order and $\varphi_l(\lambda)$ and $\varphi_r(\lambda)$ are phase shifts on reflections from the left and right mirrors surrounding the spacer layer.

In the vicinity of a filter central wavelength, spectral dependencies of phase shifts on reflection are almost linear functions, but a steepness of each dependence is tightly connected with a mirror structure [47]. For example, mirrors with high index outer layers have fewer steep phase shift dependencies than mirrors with low index outer layers. A spectral dependence of filter transmittance in the transition zone depends on the combination of all phase shift dependencies inside this zone. The modifications of the design technique from [42] are based on the recognition of this fact. Additional flexibility of the design procedure is achieved due to using more complicated mirrors as compared to standard quarter wave mirrors considered before, as well as to application of additional thin film materials.

Consider as an example phase properties of three 21-layer quarter wave mirrors with different outer layers. The first mirror is a standard quarter wave mirror with high index outer layer. Suppose the mirror central wavelength is 500 nm and that H and L index layers have refractive indices 2.35 and 1.45, respectively. The phase shift on reflection for this mirror is shown by the solid curve in Fig. 8. The dashed

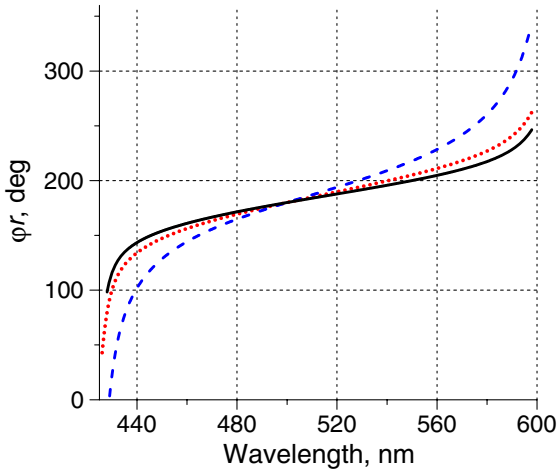

Fig. 8. (Color online) Phase shifts on reflection for three quarter wave mirrors with different upper layers: standard $HL\ldots H$ mirror (solid curve), mirror with $3H$ upper layer (dashed curve), mirror with A upper layer (dotted curve).

curve in this figure shows phase shift on reflection for the mirror with the outer H layer replaced by the layer with three quarter wave optical thickness ($3H$ layer), and the dotted curve shows phase shift on reflection for the mirror with the outer H layer replaced by the quarter wave layer with a lower refractive index of 2.05 (A layer). Using such modified mirrors instead of standard quarter wave mirrors extends opportunities for adjusting filter transmittance to the target one.

Using mirrors with $3H$ and $3L$ layers is not limited only to modifications of outer mirror layers. Such layers can also replace internal H and L layers. This allows varying phase shift steepness in a more gradual way. It is also possible to replace H and L mirror layers with A and $3A$ layers, where A stands for the quarter wave layer of additional thin film material. In a more general case, it is possible to consider not one but more additional thin film materials. Even more opportunities for optimizing a filter performance are provided by using composite spacer layers or spacer layers with additional thin film materials. For example, instead of using a $4H$ spacer layer, it is possible to consider a $2H2L$ composite spacer layer or a $4A$ spacer layer. Such substitutions vary reflectivities of mirrors surrounding filter cavities and as a consequence vary filters' performance. It should be noted that advantages of using composite filter cavities in narrow bandpass filter designs were shown more than two decades ago in [48].

The design procedure starts with specifying a filter prototype, as described in [42]. After this, the integer optimization procedure optimizes the numbers of mirror layers m_j and orders of spacer layers s_j. As soon as the integer optimization procedure is not improving filter performance any more, it is possible to expand a search performed by this procedure by adding one or more options discussed above. Different opportunities provided by these options are tested by the trial and error method, and integer optimizations are applied again and again. By combining different options, different filter designs can be obtained. Thus, multiple solutions to design problem can be obtained by specifying different numbers of filter cavities, by using different filter prototypes, and by applying different options discussed above.

As an example, illustrating the introduced modifications of the method from [42], we consider designing a bandpass filter with the central wavelength of 500 nm and the bandwidth of about 40 nm at the 50% transmittance level. For this filter we specify the bandwidth of the transmission zone at the –0.5 dB attenuation level as 36 nm and the bandwidth at the –30 dB attenuation level as 48 nm. We consider materials with refractive indices 2.35 and 1.45 as high index and low index materials (H and L materials) and material with refractive index 2.05 as an additional material (A material). The substrate has refractive index 1.52.

The ratio of specified bandwidth values (shape factor) is equal to 4/3. To achieve this shape factor with the specified H and L materials at least seven filter cavities are required. (The estimation of required number of filter cavities is discussed in detail in [42].) In Figs. 9 and 10, we present only two filter designs with the numbers of cavities equal to 9. In fact many more designs with numbers of cavities equal to 7, 8, 9 and so on and with spectral performances close to those shown in Figs. 9 and 10 can be obtained.

The design with layer optical thicknesses shown in the right part of Fig. 9 demonstrates an application of mirrors with $3H$ and $3L$ layers. Filter cavities are formed by layers with the numbers 2, 6, 12, 19, 25, 31, 38, 44, 48. Layers with the numbers 3 and 47 are $3H$ layers and layers with the numbers 8 and 42 are $3L$ layers. The last two design layers are nonquarter wave layers, which are connected with adding of AR layers at the top of a filter design constructed by the integer optimization procedure.

The design with layer optical thicknesses shown in the right part of Fig. 10 uses layers of additional thin film material. Its cavities are formed by layers with the numbers 3, 9, 17, 24, 30, 36, 43, 51, 57, four of them being A material spacer layers. There are also four A material mirror layers (layers number 1, 15, 45, 59). As before, the last two design layers are nonquarter wave layers providing AR properties in the filter transmission zone.

It should be noted that design opportunities presented by using additional filter materials and three quarter wave mirror layers were intensively used by Baumeister in a series of works devoted to designing of WDM filters and multicavity bandpass filters for visible band [49–51]. A principal difference of the considered design technique from the approach presented in these works is that there is no necessity to start designing with constructing of a microwave filter prototype, which is a key element of Baumeister's approach. Instead of this the integer optimization procedure directly fits a target filter performance by varying mirrors and spacer layers optimization parameters.

In Section 1, we mentioned an amazing success of the design approach based on the theory of equivalent layers. Analyzing a variety of designs presented in the book written by Thelen [2], one can conclude

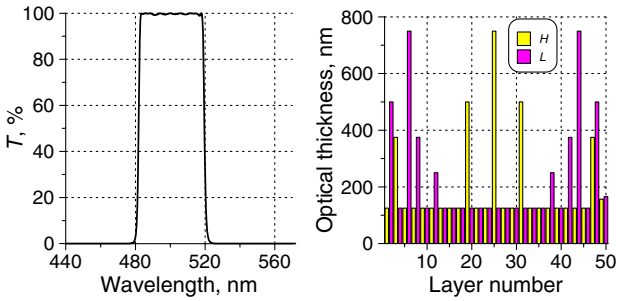

Fig. 9. (Color online) Spectral transmittance of the nine-cavity two-material bandpass filter (left) and layer optical thicknesses of this filter (right).

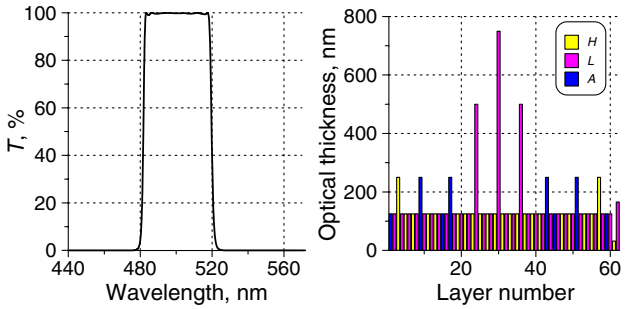

Fig. 10. (Color online) Spectral transmittance of the nine-cavity three-material bandpass filter (left) and layer optical thicknesses of this filter (right).

that from a formal point of view the design approach optimizes a series of continuous parameters providing a proper adjustment of equivalent indices of groups of layers and a series of integer parameters specifying lengths of sequences of these groups of layers. In other words, one can consider results obtained by this design approach as results of optimization of a design formula with respect to continuously varying parameters and parameters that may take only integer values.

Designing of coatings using the theory of equivalent layers requires not only a deep knowledge of this theory but also an acquaintance with many other theoretical results and tricks [2]. At the same time an outstanding power of modern computers enables developing of design techniques based on a direct optimization of design formula representation. Such optimization is performed with respect to continuously varying parameters and with respect to integer parameters included in a design formula. Below we consider two examples of a direct optimization of design formula.

The first example is designing of a multilayer mirror with the suppressed second high reflection zone. The high reflection zone for this mirror is 920–1100 nm and the high transmission region extends from 250 to 870 nm. Standard quarter wave mirrors covering the requested high reflection zone have second high reflection zones at the short wavelength part of the specified high transmission region. Originally, problems of the considered type were solved using rugate filter designs [52–54]. The so-called digital representations of rugate designs by sequences of a great number of very thin low and high index layers is also possible [55]. It was then shown that all such problems can be successfully solved by the needle optimization technique, and two-component multilayer designs featuring rugate filters properties can be obtained [21,56,57]. Alternatively a special design technique for designing of quasirugate filters can be also applied [57]. Such filters do not have thin layers at the expense of using layers with intermediate refractive index values [57].

According to the maximum principle, in thin film optics in the case of normal light incidence the best approximations of requested target dependencies are provided by two-component multilayer designs [30]. In the left part of Fig. 11 the spectral transmittance of such a 68-layer filter obtained by the needle optimization technique is depicted. Layer optical thicknesses of this filter are shown in the right part of Fig. 11. Layer materials with refractive indices 2.35 and 1.45 are used for designing. The substrate refractive index is 1.52. The design total optical thickness is equal to 5470.2 nm. Increasing this thickness one can obtain better and better results.

Layer optical thicknesses of the design in Fig. 11 form a quasiperiodic structure with three-layer combinations resembling layer combinations of the equivalent layers theory. One can check that optical thicknesses of these combinations of high index–low index–high index and low index–high index–low index layers are close to 250 nm, i.e., they are close to a quarter of the central wavelength of the requested high reflection zone. Using design formula optimization we can obtain designs that have identical groups of layers. Of course this can be achieved only due to a somewhat worse approximation of the target spectral dependence as compared to that shown in the left part of Fig. 11.

The following formula was chosen for a direct optimization of its parameters:

$$c_1Hc_2Lc_3H(a_1La_2Ha_1La_1Ha_2La_1H)^m \times a_1La_2Ha_1Ld_1Hd_2L. \quad (4)$$

The parameters a_1, a_2, c_1, c_2, c_3, d_1, d_2 of this formula are continuously varying parameters, and the parameter m is an integer parameter. In the course of optimization, continuously varying parameters are allowed to vary in the range from 0.01 to 0.50 while the integer parameter can take any integer value between 5 and 25. Control wavelength for H and L quarter wave layer optical thicknesses is taken equal to 1000 nm. In order to provide quarter wave optical thicknesses of three-layer combinations, the parameter a_2 is tightly bounded to the parameter a_1 by the equation

$$a_2 = 1 - 2a_1. \quad (5)$$

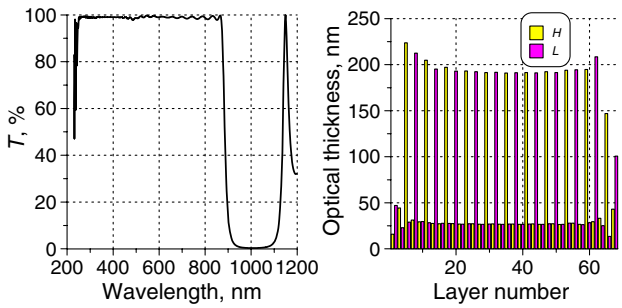

Fig. 11. (Color online) Spectral transmittance of the 68-layer two-material filter obtained by the needle optimization procedure (left) and layer optical thicknesses of this filter (right).

The following values of optimized parameters were found by the optimization procedure:

$$m = 10, \quad a_1 = 0.109, \quad c_1 = 0.060, \quad c_2 = 0.186,$$
$$c_3 = 0.176, \quad d_1 = 0.138, \quad d_2 = 0.399. \tag{6}$$

Layer optical thicknesses of the obtained design are shown in the right part of Fig. 12, and its spectral transmittance is presented in the left part of this figure. It is worth noting that the refinement of the obtained design without constraints applied by Eq. (4) gives exactly the same design as depicted in Fig. 11.

The next example of a direct formula optimization is designing a wide band high reflecting coating. The target reflectance of 100% is set in the spectral region from 400 to 900 nm with a 0.5 nm wavelength step. Refractive indices of H and L materials and substrate refractive index are the same as before. The following formula describes the designed high reflecting coating:

$$c_1 H d_1 L (a_1 H b_1 L)^{m_1} c_2 H d_2 L (a_2 H b_2 L)^{m_2} \times c_3 H d_3 L (a_3 H b_3 L)^{m_3} c_4 H. \tag{7}$$

In Eq. (7), m_1, m_2, m_3 are integer variables specifying numbers of pairs of high and low refractive index layers in respective brackets. Lower and upper limits for all m_j are set as 5 and 14, respectively. All other parameters are continuously varying parameters with the lower constraints for a_j, b_j equal to 0.8 and lower constraints for c_j, d_j equal to 0. Upper constraints for all these parameters are taken equal to 2. Control wavelength for specifying quarter wave layer optical thicknesses is 500 nm.

The considered design problem has multiple solutions that can be obtained by applying different additional constraints to optimized parameters in Eq. (7). Table 2 presents parameters of only five designs but many more designs with other N and TOT values can be easily constructed. For all designs from Table 2, average reflectance in the 400–900 nm spectral region exceeds 99.99%. Minimum reflectance values in this region are presented in the first row of Table 2. They are 99.80% and higher. Additional constraints applied in the course of design formula optimization are indicated in Table 2. For example, the notation $= a_1$ in the b_1 row of this table means that in Eq. (7) b_1 was taken equal to a_1.

Table 2. Parameters of Five Wide Band Reflector Designs

Parameters\Design	1	2	3	4	5
R_{min}, %	99.80	99.81	99.94	99.92	99.87
N	73	83	85	83	82
TOT, nm	11285.6	13045.3	13056.3	12732.0	12661.8
m_1	11	14	13	12	10
m_2	8	11	12	13	14
m_3	14	13	14	13	14
a_1	0.888	0.906	1.657	0.897	0.894
a_2	1.202	1.208	1.196	1.180	1.179
a_3	1.512	1.604	0.904	1.581	1.573
b_1	0.908	$= a_1$	1.482	$= a_1$	$= a_1$
b_2	1.168	$= a_2$	1.181	$= a_2$	$= a_2$
b_3	1.578	$= a_3$	$= a_3$	$= a_3$	$= a_3$
c_1	1.035	1.070	1.782	0.552	0.966
c_2	1.146	1.489	1.198	2.0	0.932
c_3	0.991	$= a_2$	1.263	1.509	1.494
c_4	2.0	1.982	1.961	0.100	$= 0$
d_1	0.938	1.752	1.681	0.843	0.847
d_2	1.308	1.282	1.007	1.964	0.515
d_3	0.899	1.918	$= a_3$	$= a_3$	$= a_3$

The left part of Fig. 13 presents reflectance of the design with parameters indicated in the fourth column of Table 2. Layer optical thicknesses of this design are shown in the right part of Fig. 13. All other designs also have excellent spectral properties.

4. Design Approaches Aimed at Reducing the Influence of Noncorrelated Thickness Errors

It has been an old dream to include at least some additional demands for choosing a practically optimal design in formulations of design problems [58]. It would be especially desirable to do this with respect to the demand of low sensitivity of coating design to manufacturing errors. In the case of optical monitoring techniques, manufacturing errors are correlated by a monitoring procedure, and it is impossible to describe these errors mathematically prior to starting real deposition runs or computational manufacturing experiments simulating these runs. But in

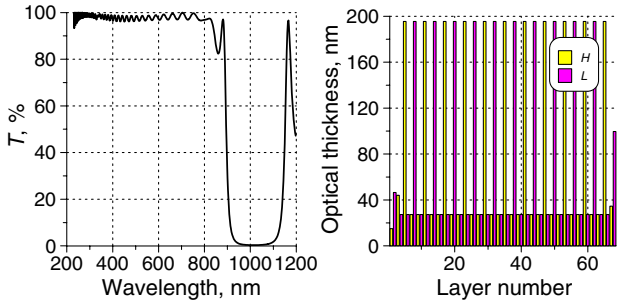

Fig. 12. (Color online) Spectral transmittance of the 68-layer two-material filter obtained by the design formula optimization (left) and layer optical thicknesses of this filter (right).

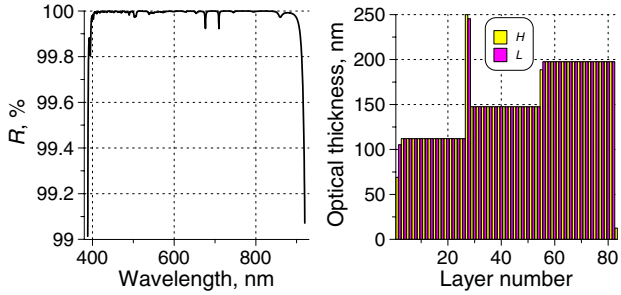

Fig. 13. (Color online) Reflectance of the wide band high reflecting mirror obtained by the design formula optimization (left) and layer optical thicknesses of this mirror (right).

the case of stable deposition processes and well-calibrated monitoring by time or quartz crystal monitoring, one can consider thickness errors in different layers as noncorrelated random errors. It is typical to assume that these errors are normally distributed with zero mathematical expectations. With these assumptions several design approaches aimed at reducing the influence of noncorrelated thickness errors have been proposed [59–63].

In [59] a modification of genetic algorithm called memetic algorithm was applied to designing of chirped-mirrors. To reduce a design sensitivity to thickness errors, a stochastic quasi-gradient local refinement taking into account these errors was included in the design procedure. An entirely deterministic design approach taking into account thickness errors was proposed in [60,61]. This approach is based on minimizing of the merit function maximum found in the design neighborhood specified by thickness errors. It can be considered as a generalization of local descent optimization procedure. As any local optimization technique it requires specification of a starting design. In [61] one can find an example of application of the proposed technique to the design of 21-layer AR coating for the visible.

A global optimization procedure that doesn't require any starting design and that takes into account a demand of reduced sensitivity to thickness errors is described in [62,63]. It is based on a simultaneous optimization of multiple designs from a neighborhood of a main pivotal design. A set of these designs called design cloud is constructed by introducing random errors in layer thicknesses of a pivotal design. A generalization of the gradual evolution version of the needle optimization technique is applied to the minimization of composite merit function that simultaneously estimates spectral characteristics of a pivotal design and all perturbed designs from a design cloud. In the course of design procedure the design cloud is renewed from time to time by generating new sets of thickness errors. This is done for preventing an adaptation of the design procedure to specific sets of errors.

The described procedure referred to as robust optimization has been successfully applied to designing of coatings of different types, including various types of dispersive mirrors [63,64]. Below we present an example of practical AR coating obtained with the help of this procedure. The AR coating is designed to reduce reflectance in the spectral region from 380 to 720 nm. The target zero reflectance values are specified in this region with the 2 nm wavelength step. The merit function *MF* estimates a root mean square deviation of design reflectance from the target reflectance in percentage. Substrate and layer refractive indices are 1.52, 2.35, 1.45 as before. Figure 14 presents refractive index profiles of four AR designs with the names AR-6, AR-10, AR-14, and AR-robust. The first three designs are "classical" AR designs [24] obtained by the standard version of the gradual evolution technique. The AR-robust

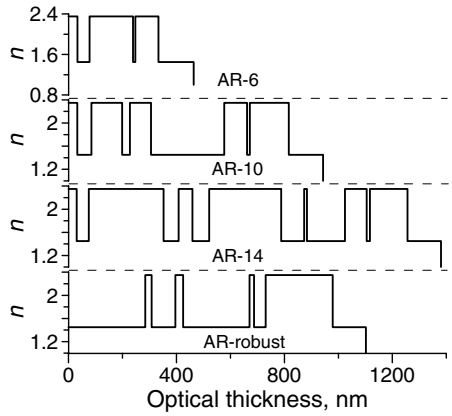

Fig. 14. Refractive index profiles of four AR coating designs: designs AR-6, AR-10, AR-14 are "classical" AR designs, design AR-robust is the design obtained using robust optimization.

design is a "practical" AR design obtained using the robust optimization. Main parameters of all four designs are provided in Table 3.

It is seen in Fig. 14 that the AR-robust design is noticeably different from other designs featuring typical cluster structures of optimal AR designs [24,65]. It is interesting to note that its structure resembles structures of AR-hard designs proposed in [26–28]. To obtain the AR-robust design, the following parameters were used by the robust optimization procedure. It was assumed that errors in layer thicknesses can be represented as a sum of two types of randomly distributed values, the first ones being absolute errors in layer thicknesses and the second ones being relative errors in layer thicknesses. Therefore layer thicknesses of a perturbed design have the form

$$\tilde{d}_j = d_j + \Delta_j + (\delta_j/100\%)d_j, \tag{8}$$

where Δ_j and δ_j are normally distributed random values with zero mathematical expectations and standard deviations σ_{abs} and σ_{rel}. In the following text these standard deviations are called levels of absolute and relative errors in layer thicknesses. It worth noting that for the production with quartz crystal monitoring such form of thickness errors representation was used and experimentally investigated in [34].

The AR-robust design was obtained with the assumption that σ_{abs} equals 1 nm and σ_{rel} equals 1%. These values are close to those experimentally found in [34]. The number of designs in a cloud was taken

Table 3. Parameters of Four AR Designs

Parameters\Design	AR-6	AR-10	AR-14	AR-Robust
N	6	10	14	9
TOT, nm	463.8	943.1	1380.0	1102.1
MF	0.263	0.135	0.129	0.169
E(MF)	0.343	0.295	0.372	0.277

equal to 20. The design procedure was started without any starting design and was interrupted when total optical thicknesses of designs exceeded 2000 nm.

The design procedure is a nonmonotonic optimization procedure due to its stochastic features (renewal of a design cloud) and also because of some basic features of the gradual evolution version of the needle optimization technique [21]. With the growing total optical thickness of a design and with the growing number of design layers, the influence of thickness errors on the composite merit function grows, and its value typically stops decreasing when some *TOT* and *N* values are achieved. This is a reflection of the trade-off between design complexity and additional demand of low sensitivity to thickness errors. For the considered design problem the best value of composite merit function is achieved with $TOT = 1102.1$ nm and $N = 9$. The achieved value of composite merit function is 0.279. It is necessary to note that one should treat this value as some estimation because it may change noticeably when a design cloud is renewed. A more accurate estimation of the AR-robust design sensitivity to noncorrelated thickness errors is provided below.

In Table 3 values of the standard merit function of all four AR designs are presented. Recall that these values represent root mean square deviations of design reflectances from the target reflectance in percentage. The *MF* value of the AR-robust design is better than that of the AR-6 design but is worse than *MF* values of the AR-10 and AR-14 designs. It is, however, necessary to compare the AR-robust design with the classical AR designs, taking into account their sensitivities to thickness errors. It is most reasonable to do this for the AR-robust and AR-10 designs that have close *N* and *TOT* values. For this comparison we take the same levels of absolute and relative errors in layer thicknesses as in the course of robust optimization, i.e., σ_{abs} is equal to 1 nm and σ_{rel} is equal to 1%.

It has been recently shown that reliable estimations of a design sensitivity to random errors may require thousands of statistical tests [35]. We have performed the error analysis with 10,000 tests for all AR designs. Figure 15 presents results of this analysis for the AR-robust (left) and AR-10 (right) designs. Solid curves in this figure show reflectances of the nonperturbed designs, dashed curves are mathematical expectations of design reflectances calculated based on the performed statistical tests, and gray areas designate corridors of deviations in which reflectance values of the perturbed designs belong with the probability of 68.3%. Figure 15 clearly demonstrates that the AR-robust design is less sensitive to thickness errors than the AR-10 design.

The last row in Table 3 presents mathematical expectations for merit function values of the perturbed AR designs. These expectations designated as *E(MF)* are also calculated on the basis of 10000 tests for each design. One can see that the *E(MF)* value for the AR-robust design is noticeably lower than the *E(MF)* value for the AR-10 design. Thus all presented results clearly demonstrate superiority of the AR-robust design over AR-10 design in the presence of thickness errors.

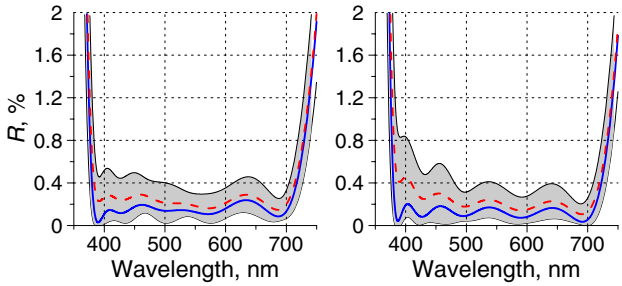

Fig. 15. (Color online) Influence of thickness errors on the reflectances of the designs AR-robust (left) and AR-10 (right).

5. Conclusion

A new paradigm in optical coating designing proposes searching not for a formally optimal design with the lowest possible merit function value but for the most practical design that has a reasonably low *MF* value and at the same time satisfies a number of additional demands facilitating its practical implementation. The gradual evolution version of the needle optimization technique enables constructing a set of designs with various combinations of the three main design parameters *MF*, *N*, and *TOT*. Having at their disposal such a set of designs with decreasing *MF* values and increasing *N* and *TOT* values helps the designers to find a reasonable correlation between an accuracy of approximation of target spectral dependencies and design complexity. Because of this fact and also because of its outstanding computational efficiency, the gradual evolution version of the needle optimization technique can be considered as the most general design technique. There are however additional parameters that may influence a choice of the most practical design, and other techniques may be well-suited for solving specific design problems.

In this paper we discussed several developments in design techniques that we consider as important ones in a view of the new design paradigm. In different application areas there are design problems with low and upper constraints for allowed values of coating layer thicknesses. For such problems a special stochastic optimization procedure that directly takes into account thickness constraints can be applied. Because of effective optimization routines this procedure is able to perform thousands of optimizations and to select excellent designs with several dozens of layers in a quite reasonable time. Along with taking into account thickness constraints, there is one more reason for application of the proposed stochastic procedure. It turns out that many design problems have multiple solutions with close combinations of the three main design parameters *MF*, *N*, and *TOT*. The proposed procedure is aimed at

obtaining such solutions which presents additional opportunities for choosing of a practically optimal design.

Taking into account additional practical demands may require application of special design techniques involving integer optimization. In this paper we considered two types of such techniques. The first one is aimed at designing multicavity narrow bandpass filters with quarter wave or multiple quarter wave layer optical thicknesses. It is a modification of our technique that was initially applied for designing of filters for WDM applications. The proposed modification allows using three quarter wave mirror layers, additional materials for mirror layers, composite spacer layers or spacer layers of additional materials. It dramatically extends designers' opportunities in constructing bandpass filters with extremely steep transmittance slopes, bandwidths of several tens of nanometers, and very small ripples in transmission zones. The second technique involving integer optimization is aimed at covering design problems that have been traditionally solved using the theory of equivalent layers. An outstanding power of modern computers and modern optimization routines enable direct optimizations of design formula representations. We considered two examples of direct optimizations of design formulas that demonstrate a practical significance of this technique.

One more technique considered in this paper is aimed at reducing the influence of noncorrelated thickness errors on design spectral characteristics. It is based on a simultaneous optimization of multiple designs that are obtained from a main pivotal design by introducing random errors in its layer thicknesses. A generalization of the gradual evolution version of the needle optimization technique is applied to the minimization of composite merit function that simultaneously estimates spectral characteristics of a pivotal design and of all perturbed designs. This generalized procedure constructs a set of robust designs that differ from classical designs obtained by the gradual evolution procedure by reduced sensitivity to thickness errors.

This work was supported by the Deutsche Forschungsgemeinschaft (DFG) Cluster of Excellence, "Munich Centre for Advanced Photonics" (http://www.munich-photonics.de) and the Russian Fund of Basic Research, projects 10-07-00480-a and 11-07-91153a.

References

1. H. A. Macleod, *Thin Film Optical Filters*, 4th ed. (CRC Press, 2010).
2. A. Thelen, *Design of Optical Interference Coatings* (McGraw-Hill, 1988).
3. S. Furman and A. V. Tikhonravov, *Basics of Optics of Multilayer Systems* (Edition Frontieres, 1992).
4. J. A. Dobrowolski, *Optical Properties of Films and Coatings* (McGraw-Hill, 1994), pp. 42.3–42.130.
5. N. Kaiser and H. K. Pulker, *Optical Interference Coatings* (Springer-Verlag, 2003).
6. P. W. Baumeister, *Optical Coating Technology* (SPIE, 2004).
7. J. A. Dobrowolski, "Numerical methods for optical thin films," Opt. Photon. News **8**(6), 24–33 (1997).
8. J. A. Dobrowolski and D. Lowe, "Optical thin film synthesis program based on the use of Fourier transforms," Appl. Opt. **17**, 3039–3050 (1978).
9. P. G. Verly, J. A. Dobrowolski, W. Wild, and R. Burton, "Synthesis of high rejection filters with the Fourier transform method," Appl. Opt. **28**, 2864–2875 (1989).
10. P. G. Verly and J. A. Dobrowolski, "Iterative correction process for optical thin film synthesis with the Fourier transform method," Appl. Opt. **29**, 3672–3684 (1990).
11. P. G. Verly, J. A. Dobrowolski, and R. R. Willey, "Fourier-transform method for the design of wideband antireflection coatings," Appl. Opt. **31**, 3836–3846 (1992).
12. P. G. Verly, "Fourier-transform technique with frequency filtering for optical thin film design," Appl. Opt. **34**, 688–694 (1995).
13. B. G. Bovard, "Rugate filter design: the modified Fourier transform technique," Appl. Opt. **29**, 24–30 (1990).
14. H. Fabricius, "Gradient-index filter: designing filters with step skirts, high reflection and quintic matching layers," Appl. Opt. **31**, 5191–5196 (1992).
15. X. Cheng, B. Fan, J. A. Dobrowolski, L. Wang, and Z. Wang, "Gradient-index optical filter synthesis with controllable and predictable refractive index profiles," Opt. Express **16**, 2315–2321 (2008).
16. J. A. Dobrowolski and R. A. Kemp, "Refinement of optical multilayer systems with different optimization procedures," Appl. Opt. **29**, 2876–2893 (1990).
17. L. Li and J. A. Dobrowolski, "Computation speeds of different optical thin-film synthesis methods," Appl. Opt. **31**, 3790–3799 (1992).
18. J. Kruschwitz, "Software tools speed optical thin-film design," Laser Focus World **39**, 157–166 (2003).
19. A. V. Tikhonravov, "Synthesis of optical coatings using optimality conditions," in *Vestnik MGU*, Vol. 23 of Physics and Astronomy Series (1982), pp. 91–93.
20. A. V. Tikhonravov, M. K. Trubetskov, and G. W. DeBell, "Application of the needle optimization technique to the design of optical coatings," Appl. Opt. **35**, 5493–5508 (1996).
21. A. V. Tikhonravov, M. K. Trubetskov, and G. W. DeBell, "Optical coating design approaches based on the needle optimization technique," Appl. Opt. **46**, 704–710 (2007).
22. J. A. Dobrowolski, "Completely automatic synthesis of optical thin film systems," Appl. Opt. **4**, 937–946 (1965).
23. A. V. Tikhonravov, M. K. Trubetskov, T. V. Amotchkina, and M. A. Kokarev, "Key role of the coating total optical thickness in solving design problems," Proc. SPIE **5250**, 312–321 (2004).
24. A. V. Tikhonravov, M. K. Trubetskov, T. V. Amotchkina, and J. A. Dobrowolski, "Estimation of the average residual reflectance of broadband antireflection coatings," Appl. Opt. **47**, C124–C130 (2008).
25. A. Tikhonravov, M. Trubetskov, and I. Kasahara, "Achievements and challenges in the design and production of high quality optical coatings," IEICE Trans Electron **E91-C**, 1622–1629 (2008).
26. U. Schulz, U. B. Schallenberg, and N. Kaiser, "Antireflection coating design for plastic optics," Appl. Opt. **41**, 3107–3110 (2002).
27. U. Schulz, U. B. Schallenberg, and N. Kaiser, "Symmetrical periods in antireflective coatings for plastic optics," Appl. Opt. **42**, 1346–1351 (2003).
28. U. Schulz, K. Lau, and N. Kaiser, "Antireflection coating with UV-protective properties for polycarbonate," Appl. Opt. **47**, C83–C87 (2008).
29. S. Wilbrandt, O. Stenzel, and N. Kaiser, "All-oxide broadband antireflection coatings by plasma ion assisted deposition: design, simulation, manufacturing and re-optimization," Opt. Express **18**, 19732–19742 (2010).
30. A. V. Tikhonravov, "Some theoretical aspects of thin film optics and their applications," Appl. Opt. **32**, 5417–5426 (1993).
31. A. V. Tikhonravov and M. K. Trubetskov, "Computational manufacturing as a bridge between design and production," Appl. Opt. **44**, 6877–6884 (2005).

32. B. Badoil, F. Lemarchand, M. Cathelinaud, and M. Lequime, "Interest of broadband optical monitoring for thin-film filter manufacturing," Appl. Opt. **46**, 4294–4303 (2007).
33. D. Ristau, H. Ehlers, S. Schlichting, and M. Lappschies, "State of art in deterministic production of optical thin films," Proc. SPIE **7101**, 71010C (2008).
34. K. Friedrich, S. Wilbrandt, O. Stenzel, N. Kaiser, and K. H. Hoffmann, "Computational manufacturing of optical interference coatings: method, simulation results, and comparison with experiment," Appl. Opt. **49**, 3150–3162 (2010).
35. A. V. Tikhonravov, M. K. Trubetskov, T. V. Amotchkina, and V. Pervak, "Estimations of production yields for choosing of a practically optimal optical coating design," Appl. Opt. **50**, C141–C147 (2011).
36. A. Zoeller, M. Boos, R. Goetzelmann, H. Hagedorn, and W. Klug, "Substantial progress in optical monitoring by intermittent measurement technique," Proc. SPIE **5963**, 105–113 (2005).
37. C.-C. Lee, K. Wu, C.-C. Kuo, and S.-H. Chen, "Improvement of the optical coating process by cutting layers with sensitive monitoring wavelengths," Opt. Express **13**, 4854–4861 (2005).
38. B. Chun, C. K. Hwangbo, and J. S. Kim, "Optical monitoring of nonquarterwave layers of dielectric multilayer filters using optical admittance," Opt. Express **14**, 2473–2480 (2006).
39. A. V. Tikhonravov and M. K. Trubetskov, "Elimination of cumulative effect of thickness errors in monochromatic monitoring of optical coating production: theory," Appl. Opt. **46**, 2084–2090 (2007).
40. A. N. Tikhonov, A. V. Tikhonravov, and M. K. Trubetskov, "Second order optimization methods in the synthesis of multilayer coatings," Comp. Maths. Math. Phys. **33**, 1339–1352 (1993).
41. J. Nocedal and S. J. Wright, *Numerical Optimization* (Springer Verlag, 2006).
42. A. V. Tikhonravov and M. K. Trubetskov, "Automated design and sensitivity analysis of wavelength-division multiplexing filters," Appl. Opt. **41**, 3176–3182 (2002).
43. A. V. Tikhonravov, M. K. Trubetskov, and T. V. Amotchkina, "Investigation of the effect of accumulation of thickness errors in optical coating production using broadband optical monitoring," Appl. Opt. **45**, 7026–7034 (2006).
44. A. V. Tikhonravov, M. K. Trubetskov, and T. V. Amotchkina, "Investigation of the error self-compensation effect associated with broadband optical monitoring," Appl. Opt. **50**, C111–C116 (2011).
45. H. A. Macleod, "Turning value monitoring of narrow-band all-dielectric thin film optical filters," Opt. Acta **19**, 1–28 (1972).
46. A. V. Tikhonravov, M. K. Trubetskov, I. V. Kozlov, V. G. Zhupanov, and E. V. Klyuev, "Design and production of bandpass filters with steep transmittance slopes," in *Optical Interference Coatings Topical Meeting* (Optical Society of America, 2010), paper MA6.
47. A. V. Tikhonravov, P. W. Baumeister, and K. V. Popov, "Phase properties of multilayers," Appl. Opt. **36**, 4382–4392 (1997).
48. W. H. Southwell, W. J. Gunning, and R. L. Hall, "Narrow-bandpass filter using partitioned cavities," Proc. SPIE **678**, 177–184 (1986).
49. P. W. Baumeister, "Design of a wavelength-division multiplexing bandpass with quasi-chebyshev spectral shape," Appl. Opt. **40**, 1132–1137 (2001).
50. P. Baumeister, "Design of a coarse WDM bandpass filter using the Thelen bandpass design method," Opt. Express **9**, 652–657 (2001).
51. P. Baumeister, "Application of microwave technology to design an optical multilayer bandpass filter," Appl. Opt. **42**, 2407–2414 (2003).
52. W. H. Southwell and R. L. Hall, "Rugate filter sidelobe suppression using quintic and rugated quintic matching layers," Appl. Opt. **28**, 2949–2951 (1989).
53. W. H. Southwell, "Using apodization functions to reduce sidelobes in rugate filters," Appl. Opt. **28**, 5091–5094 (1989).
54. B. G. Bovard, "Rugate filter theory: an overview," Appl. Opt. **32**, 5427–5442 (1993).
55. W. H. Southwell, "Coating design using very thin high- and low-index layers," Appl. Opt. **24**, 457–460 (1985).
56. V. Pervak, A. V. Tikhonravov, M. K. Trubetskov, J. Pistner, F. Krausz, and A. Apolonski, "Band filters: 2-material technology versus rugate," Appl. Opt. **46**, 1190–1193 (2007).
57. A. V. Tikhonravov, M. K. Trubetskov, and T. V. Amotchkina, "Application of constrained optimization to the design of quasi-rugate optical coatings," Appl. Opt. **47**, 5103–5109 (2008).
58. A. Thelen, "Design of a hot mirror: contest results," Appl. Opt. **35**, 4966–4977 (1996).
59. V. Yakovlev and G. Tempea, "Optimization of chirped mirrors," Appl. Opt. **41**, 6514–6520 (2002).
60. O. Nohadani, J. R. Birge, F. X. Kärtner, and D. J. Bertsimas, "Robust chirped mirrors," Appl. Opt. **47**, 2630–2636 (2008).
61. J. R. Birge, F. X. Kärtner, and O. Nohadani, "Improving thin-film manufacturing yield with robust optimization," Appl. Opt. **50**, C36–C40 (2011).
62. M. K. Trubetskov and A. V. Tikhonravov, "Robust synthesis of multilayer coatings," in *Optical Interference Coatings Topical Meeting* (Optical Society of America, 2010), paper TuA4.
63. V. Pervak, M. K. Trubetskov, and A. V. Tikhonravov, "Robust synthesis of dispersive mirrors," Opt. Express **19**, 2371–2380 (2011).
64. V. Pervak, O. Pronin, O. Razskazovskaya, J. Brons, I. B. Angelov, M. K. Trubetskov, A. V. Tikhonravov, and F. Krausz, "High-dispersive mirrors for high power applications," Opt. Express **20**, 4503–4508 (2012).
65. J. A. Dobrowolski, A. V. Tikhonravov, M. K. Trubetskov, B. T. Sullivan, and P. G. Verly, "Optimal single-band normal incidence antireflection coatings," Appl. Opt. **35**, 644–658 (1996).